THE JOURNAL OF BIOLOGICAL CHEMISTRY
Vol. 278, No. 31, Issue of August 1, pp. 29231–29239, 2003
Printed in U.S.A.

Syntaxin 1A Modulates the Voltage-gated L-type Calcium Channel ($Ca_v1.2$) in a Cooperative Manner*

Received for publication, February 10, 2003, and in revised form, April 28, 2003
Published, JBC Papers in Press, April 29, 2003, DOI 10.1074/jbc.M301401200

Hadar Arien‡, Ofer Wiser‡, Isaiah T. Arkin, Hadas Leonov, and Daphne Atlas§

From the Institute of Life Sciences, Department of Biological Chemistry, The Hebrew University of Jerusalem, Jerusalem 91904, Israel

Syntaxin 1A (Sx1A) modifies the activity of voltage-gated Ca^{2+} channels acting via the cytosolic and the two vicinal cysteines (271 and 272) at the transmembrane domain. Here we show that Sx1A modulates the Lc-type Ca^{2+} channel, $Ca_v1.2$, in a cooperative manner, and we explore whether channel clustering or the Sx1A homodimer is responsible for this activity. Sx1A formed homodimers but, when mutated at the two vicinal transmembrane domain cysteines, was unable to either dimerize or modify the channel activity suggesting disulfide bond formation. Moreover, applying global molecular dynamic search established a theoretical prospect of generating a disulfide bond between two Sx1A transmembrane helices. Nevertheless, Sx1A activity was not correlated with Sx1A homodimer. Application of a vicinal thiol reagent, phenylarsine oxide, abolished Sx1A action indicating the accessibility of Cys-271,272 thiols. Sx1A inhibition of channel activity was restored by phenylarsine oxide antidote, 2,3-dimercaptopropanol, consistent with thiol interaction of Sx1A. In addition, the supralinear mode of channel inhibition was correlated to the monomeric form of Sx1A and was apparent only when the three channel subunits $\alpha_1 1.2/\alpha_2\delta 1/\beta 2a$ were present. This functional demonstration of cooperativity suggests that the three-subunit channel responds as a cluster, and Sx1A monomers associate with a dimer (or more) of a three-subunit Ca^{2+} channel. Consistent with channel cluster linked to Sx1A, a conformational change driven by membrane depolarization and Ca^{2+} entry would rapidly be transduced to the exocytotic machinery. As shown herein, the supralinear relationship between Sx1A and the voltage-gated Ca^{2+} channel within the cluster could convey the cooperativity that distinguishes the process of neurotransmitter release.

Signal transduction in the synapse is initiated by neurotransmitter release as a consequence of fusion that takes place between synaptic vesicles and the plasma membrane. It is commonly accepted that at the heart of this tightly regulated, multifarious process lies the ternary complex formed by the synaptic proteins syntaxin 1A (Sx1A),[1] SNAP-25, and synaptobrevin II (1–3). This ternary complex is thought to be responsible for juxtaposing the synaptic vesicle and the plasma membrane prior to membrane fusion, which involves the binding of soluble *N*-ethylmaleimide-sensitive factor (NSF) (1–3). It is for this reason that the above-mentioned ternary complex is referred to as the SNARE (receptor for soluble NSF attachment proteins) complex.

Analysis of ternary complexes formed by the full-length proteins revealed that the C-terminal transmembrane domains (TMDs) of both Sx1A and synaptobrevin II were protected from trypsin digestion (4). Moreover, inclusion of these TMDs increased the stability of the ternary complexes and affected the ability of the cytoplasmic domains to join other proteins (4, 5). Co-reconstituted into liposomes, synaptobrevin II and syntaxin 1A formed a stable binary complex that required the presence of the TMDs (6).

The two SNAREs, Sx1A and synaptobrevin, are both type II bitopic membrane proteins, defined by an N-terminal cytoplasmic region and a single transmembrane domain (7, 8). Highly conserved oligomerization motifs have been identified in the transmembrane domains of Sx1A and synaptobrevin II in studies using the nuclease A/fusion proteins (9, 10). These motifs contribute to the interaction between the two proteins in forming homodimers (syntaxin/syntaxin and synaptobrevin II/synaptobrevin II) as well as a heterodimer complex (syntaxin/synaptobrevin II). These interactions serve as further examples in which transmembrane domains participate in the sequence-specific assembly of integral membrane proteins.

Sx1A has also been shown to modify the kinetic properties of voltage-gated Ca^{2+} channels establishing a pivotal role of Ca^{2+} channels in the onset and regulation of the release process (11–13). The TMD of syntaxin 1A participates in the reduction of current amplitude of N-type ($Ca_v2.2$) and Lc-type ($Ca_v1.2$) channels (12, 13). A Sx1A chimera in which the TMD domain was switched with syntaxin 2 TMD abolished the inhibitory effect of Sx1A, thereby pointing to the inhibitory function of the transmembrane domain (12, 13). Furthermore, botulinum toxin C1, shown to cleave specifically Sx1A close to its transmembrane anchor, abolished Sx1A modulation of inward currents, most likely by uncoupling the Sx1A/channel interaction (12).

The Sx1A TMD harbors two vicinal cysteines Cys-271 and Cys-272, one of which, Cys-271, is part of the aforementioned dimerization motifs (10). The two cysteines appear to play an essential role in modulating the voltage-gated channels, $Ca_v1.2$ and $Ca_v2.2$ (12, 13). In contrast, syntaxin 2, which has valine residues in the TMD in place of the two cysteines, does not modulate the channel activity (11, 12). A Sx1A mutant in which the two cysteines were mutated to valine showed loss

* This work was supported by a grant from the Penn Foundation and the H. L. Lauterbach Fund (to D. A.). The costs of publication of this article were defrayed in part by the payment of page charges. This article must therefore be hereby marked "*advertisement*" in accordance with 18 U.S.C. Section 1734 solely to indicate this fact.

‡ Both authors contributed equally to this work.

§ To whom correspondence should be addressed. Tel.: 972-2-658-5406; Fax: 972-2-658-5413; E-mail: datlas@vms.huji.ac.il.

[1] The abbreviations used are: Sx1A, syntaxin 1A; TMD, transmembrane domain; SNARE, soluble *N*-ethylmaleimide-sensitive factor attachment protein receptor; DTT, dithiothreitol; PAO, phenylarsine oxide; wt, wild type; r.m.s.d., root mean square deviation; BAL, British anti-Lewisite.

of function, with no effect on current amplitude, whereas mutating only one of the two cysteines retained the inhibitory activity of syntaxin (12). A gain of function was obtained when the two valines of syntaxin 2 TMD were mutated to Cys, providing the mutant with the ability to inhibit inward Ba^{2+} currents. Voltage-activated calcium channels are heteromeric complexes composed of the pore-forming α_1 subunit together with accessory $\alpha_2\delta$ and β subunits. Whole-cell Ca^{2+} channel currents are increased by either $\alpha_2\delta$ or β2a subunits, up to 100-fold by both. Co-expression of $\alpha_2\delta$ (either with or without β) triples the channel density on the cell membrane, whereas expression of β2a increases the open state probability (P_o) (14). The α_1 subunit contains binding sites for pharmacological agents, proteins, or toxins and determines the electrophysiological properties of different types of Ca^{2+} channels (15–25) as well as interaction sites with Sx1A, SNAP-25, and synaptotagmin (26–34). The II–III linker of the α_1 subunit was suggested to be the docking site of exocytotic vesicles (13, 29–31, 34). The Sx1A modulation of the activity of the channel heterocomplex could perhaps represent an interaction of more than one oligomer, composing a complicated relationship. As such, in order to better understand the mechanism of Sx1A modulation of the activity of the channel we tested the following: 1) the functional implication of putative Sx1A homodimers and monomers to their interaction with the voltage-gated Ca^{2+} channels ($Ca_v1.2$) by reconstituting the Sx1A wt and mutants in the *Xenopus* oocytes expression system; 2) the contribution of Sx1A transmembranal cysteines to modulating channel activity when Ca^{2+} ions are the charge carrier; 3) The consequences of thiol groups at the Sx1A TMD to its interaction with the channel; 4) the Sx1A non-linear inhibition of channel activity. Finally, we discuss Sx1A homodimer formation and the contribution of structural plasticity of Sx1A TMD segments to channel clustering; and we propose channel clusters as a model to explain the distinct cooperativity at the late step of membrane fusion.

EXPERIMENTAL PROCEDURES

Isolation of Xenopus Oocytes and cRNA Injection—Stage V and VI oocytes were surgically removed from female *Xenopus laevis* and treated for 1.5–2 h with 2 mg/ml collagenase (154 units/mg, Worthington) in a Ca^{2+}-free ND solution (mM): 96 NaCl, 2 KCl, 1 $MgCl_2$, 5 HEPES, pH 7.4. After a 12-h recovery period, completely defolliculated oocytes were injected with cRNA mixtures of channel subunits. One day later, cRNA of Sx1A or control (water) was injected (see below and see Refs. 11 and 31). Oocytes were kept at 19 °C for 4–8 days before protein expression was determined.

cDNA Constructs—$\alpha_1$1.2 (dN60-del1773; X15539) and rat β2a (m80545) were obtained from Dr. N. Qin and Dr. L. Birnbaumer (University of North Carolina); α_2/δ1 rabbit skeletal (M86621) from A. Schwartz (University of Ohio). *In vitro* transcription kit was from Stratagene.

cRNA Injection into Oocytes—cRNAs were made using the T7/T3 Stratagene kit, and the product was monitored by gel electrophoresis and optical density measurements. cRNA mixtures were injected into oocytes using a digital microdispenser (Drummond 510, Broomel, PA), in a final volume of 40 nl. Oocytes were kept in 19 °C for 4–8 days until the protein expression was assayed. cRNA amounts were adjusted empirically to make the inward current lower than −4 μA. A relatively high amount of $\alpha_1$1.2 cRNA was injected when expressed alone for improved resolution of Sx1A inhibition of current amplitude. cRNA amounts are as follows: 7 ng/oocyte of $\alpha_1$1.2 when injected alone; 3 ng/oocyte of $\alpha_1$1.2 and 5 ng/oocyte of β2a; 3 ng/oocyte of $\alpha_1$1.2 and 2 ng/oocyte of $\alpha_2\delta$1; 2 ng/oocyte of $\alpha_1$1.2, 1.5 ng/oocyte of $\alpha_2\delta$1, and 5 ng/oocyte of β2a.

Electrophysiological Assays—Whole-cell currents were recorded by applying a standard two-microelectrode voltage clamp using a Dagan 8500 amplifier. Voltage and current 1% agar cushioned electrodes (0.3–0.6-megohm tip resistance) were filled with 3 M KCl. A reference electrode was placed in a reference chamber filled with 3 M KCl and connected to the assay chamber by two glass bridges filled with 1% agarose dissolved in 3 M KCl. Prior to recording for 15–60 min, oocytes were injected with 40 nl of solution containing 5 mM HEPES, pH 7.0, and 5 mM of the Ca^{2+} chelator 1,2-bis (2-aminophenoxy) ethane-*N, N, N′, N′*-tetraacetic acid (potassium salt) final concentration (in oocyte). Current-voltage relationships were determined by applying test pulses with 5- or 10-mV increments from −80 to +60 mV by the data acquisition software Clampex version 7 (Axon Instruments, Foster City, CA). Oocytes were assayed for calcium channel activity in Ba^{2+} solution (mM): 5 Ba $(OH)_2$, 35 *N*-methyl-D-glucamine, 40 triethanolamine, 1 KOH, and 5 HEPES, pH 7.5, titrated to pH 7.5 with methyl sulfonate. Peak currents of each trace plotted against the test potentials gave a current-voltage relationship plot. The negative peak of the bell-shaped, current-voltage relationship plot of each group of oocytes was normalized relative to the group with no Sx1A expression and plotted against the concentration of Sx1A expressed in the oocyte.

Pulse duration was adjusted according to tested measurement and channel type. Time scale bars are displayed in each experiment. Current traces were leak-subtracted on-line by Clampex 7 software, and channel activation rates were analyzed by applying a mono-exponential fit of the Clampfit 6 software (Axon Instruments). Fit = $A \exp(t/\tau) + B$, where A is current amplitude, τ is time constant, and t is ms. Fit was applied from the beginning of the trace just after the capacitative transient to the peak current region. The capacitative transient lasted for 1–2.5 ms and was subtracted on-line. Hill coefficient (n_H) was determined by applying linear regression to the Hill plot.

Data Presentation and Statistical Analysis—Peak current and time constant values analyzed by Clampfit 6 and transferred as ASCI file to an Excel worksheet (Microsoft Inc.). Data were averaged for each group of oocytes, and S.E. was determined. Data are presented as means ± S.E. Statistical significance relative to the control group in each experiment was done by Student's t test by the Excel software. Statistical significance between multiple groups in each experiment was determined using one-way analysis of variance test using the Origin 5 software (Microcal). Final data was transferred to Origin 5 worksheet, plotted, and printed as final figures.

Membrane Preparation and Western Blotting—Oocytes were tested for protein expression by Western analysis 5–7 days after cRNA injection. Oocytes were homogenized in buffer containing (in mM) Tris 10, EDTA 1, sucrose 250 and addition of a mixture of proteases as follows: aprotinin, phenylmethylsulfonyl fluoride, iodoacetamide, pepstatin A, and leupeptin at 4 °C. Homogenates were centrifuged (12,000 × g, 10 min); the pellet (the yolk) was discarded, and the clear (cytosolic fraction) and the white supernatant (membrane fraction) were collected. Protein was determined by a micro-Bradford assay in enzyme-linked immunosorbent assay reader plate using bovine serum albumin as standard. Protein samples (30 μg) were mixed with 100 mM DTT and 2% SDS, boiled for 3 min, applied to 10% SDS-PAGE, transferred to nitrocellulose, and probed using affinity-purified monoclonal anti-Sx1A (Sigma) followed by a horseradish peroxidase-conjugated anti-mouse antibody. Sx1A expression was detected by enhanced chemiluminescence.

For visualizing Sx1A dimers, the samples were mixed in native protein loading buffer (no SDS and no DTT) and were not boiled. These samples were loaded on 8% SDS-PAGE and processed as mentioned above.

Global Search Molecular Dynamics—A global molecular dynamics search was performed for the Sx1A wild type and each of its mutants Sx(C271V), Sx(C272V), Sx(C271V/C272V), and in addition for syntaxin 2 wild type and its mutant Sx2(C272V/C273V). All calculations were performed using parallel version of crystallography and NMR system, the parallel-processing version of the crystallography and NMR system (CNS version 0.3) (35), with the optimized potentials for liquid simulations parameter set and united atom topology (36), explicitly describing only polar and aromatic hydrogens. A global search was conducted as described elsewhere, by using CHI (CNS searching of helical interactions), assuming a symmetrical interaction between the two helices (37). An α-helical conformation was maintained during the search by applying 3.2-Å maximal distance restraints between O_i and N_{i+4}. Calculations were performed in a simulated membrane environment with a dielectric constant of 2.0.

Trials were conducted starting from both left and right 25° crossing angles, with the helices rotated 360° about their helical axes in 5° increments. Sampling was further increased by performing six trials from each starting configuration, using different initial random velocities, making a total of 864 trials. Clusters of output structures were identified, containing 13 or more structures within 1.0-Å r.m.s.d. from any other structure within the cluster. Consequently, some clusters overlap, and output structures may be members of more than one

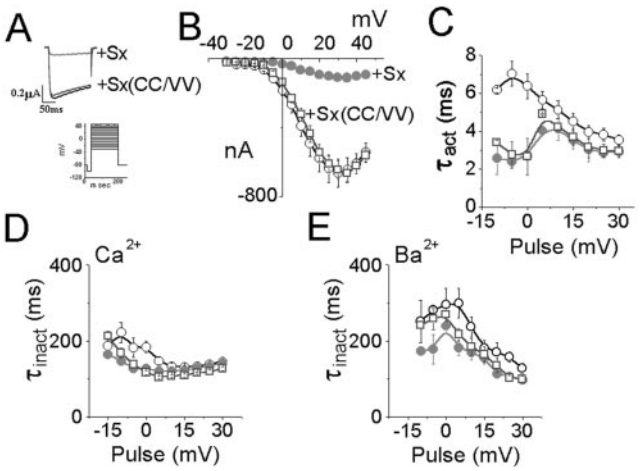

FIG. 1. **Mutation at Cys-271 and Cys-272 of Sx1A alters interaction with $Ca_v1.2$.** Oocytes were injected with $\alpha_1 1.2/\alpha_2\delta 1/\beta 2a$ at concentrations of 2, 1.5, and 5 ng/oocyte, respectively, and 24 later with Sx1A (3 ng/oocyte) or Sx1A double mutant Sx(CC/VV) (3 ng/oocyte). *A*, at day 6 after injection, Ca^{2+} currents were activated from a holding potential of −80 mV by a single voltage step of 140 ms duration to a step potential of +20 mV in oocytes expressing the three channel subunit, with and without Sx1A or Sx(CC/VV). *B*, Ca^{2+} currents were activated from −80 mV by voltage steps applied at 5-s intervals to potentials between −35 to +45mV (see *inset*). Leak-subtracted peak current-voltage relationship: collected data from oocytes expressing the three channel subunits (○) together with Sx1A (●) or syntaxin (CC/VV) (□). The data points correspond to the mean ± S.E. of current amplitude ($n = 8$). *C*, the averaged time constants of activation (τ_{act}, mean ± S.E., $n = 6$) are plotted against test pulses between −15 and +30 mV in the absence (○) and in the presence of Sx1A (●) and Sx(CC/VV) (□). *D* and *E*, the averaged time constant of inactivation (τ_{inact}, mean ± S.E., $n = 8$) in 5 mM Ca^{2+} and 5 mM Ba^{2+} are plotted against test pulses between −15 and +30mV; the channel alone (○), with Sx1A (●), and Sx(CC/VV) (□). Student's *t* test (two population) was performed, and *p* values <0.05 were obtained (see Table II).

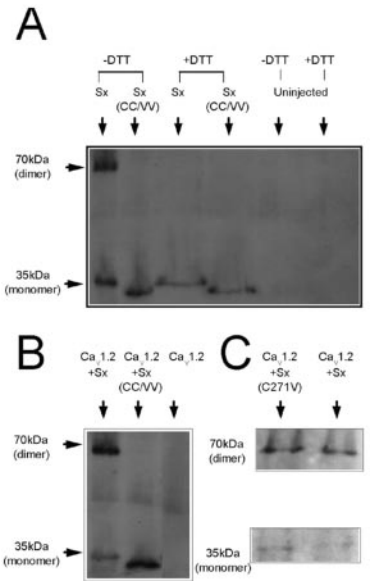

FIG. 2. **Sx1A mutant does not form homodimers.** Sx1A wt (3 ng/oocytes) and Sx(CC/VV) (3 ng/oocyte) were injected into *Xenopus* oocytes, and 5 days later lysates were prepared and proteins were separated by SDS-PAGE (10%) and visualized in a Western blot using anti Sx1A monoclonal antibody. The protein samples had no SDS and no DTT. *A*, the 70-kDa homodimer and the 35-kDa monomer of Sx1A wt was shown. Under the same experimental conditions Sx(CC/VV) was visualized only as a monomer. The Sx1A homodimer was reduced when DTT was added to the protein sample. *B*, Sx1A homodimer was apparent in lysates of oocytes co-expressing the three channel subunits along with Sx1A. *C*, the syntaxin mutant Sx(C271V) appeared as a homodimer under conditions described in *A*.

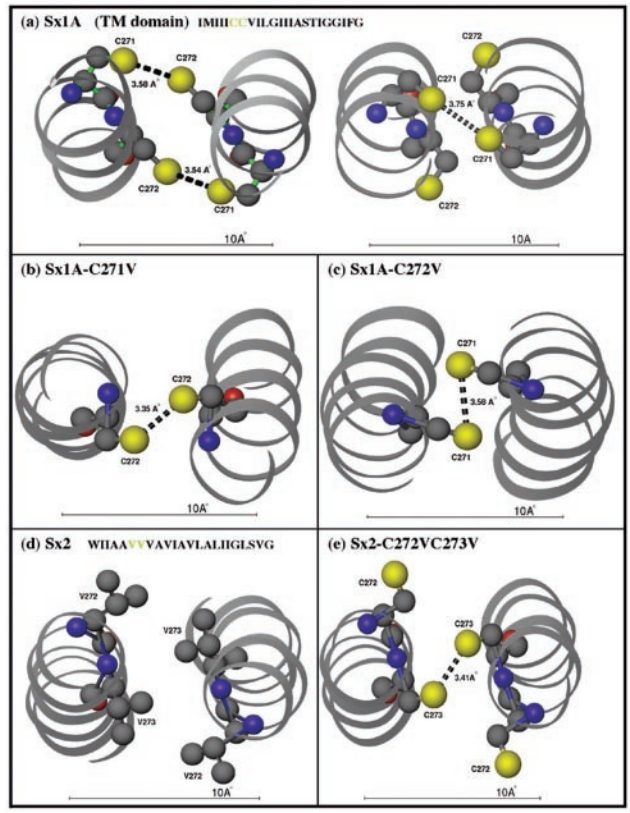

FIG. 3. **Comparisons between the average cluster structures of TMD of Sx1A (*a–c*), syntaxin 2 (*d–e*), and mutants clusters by calculating the r.m.s.d. of their backbone Cα.** *a*, results for Sx1A wild type GMDS in which out of the clusters obtained, two are shown in which disulfide bonds are possible. *b*, same as *a* except that Cys-271 is mutated to a valine. *c*, same as *a*, except that Cys-272 is mutated to a valine. *d*, the only cluster found for wild type syntaxin 2. *e*, a cluster obtained for a double mutant of syntaxin 2 TMD in which both Val-272 and Val-273 are mutated to cysteines. Atom colors are as follows: *gray*, carbon; *yellow*, sulfur; *red*, oxygen; and *blue*, nitrogen.

cluster. The output structures in a cluster were averaged and subjected to a further simulated annealing protocol, as in the initial search. This average was taken as representative of the cluster.

Analysis of the Simulations—Comparison of the average structures of clusters from the different mutants was made by calculating the r.m.s.d. of their carbon backbones. However, for Sx1A, no significant similarity was found between the clusters of different mutants, so a different approach was adopted. For each Sx1A mutant and the wild type, more specific clusters were searched for, in which the distance of the cysteine Sγs in positions 271 and/or 272 was in the range of 3–4 Å.

RESULTS

The Transmembranal Cys-271 and Cys-272 of Sx1A Play a Crucial Role in the Modulation of $Ca_v1.2$ Channel Activity—Previously we showed that mutation of two cysteines Cys-271 → Val and Cys-272 → Val abolished the ability of Sx1A to inhibit Ba^{2+} current amplitude but did not interfere with the modulation of $Ca_v1.2$ activation (12). Because the modification of channel activity by Sx1A is affected by switching the charge carrier (33), we explored the functional importance of Sx1A vicinal cysteines in Ca^{2+} as the permeating ion. Expression of the three subunits, $\alpha_1 1.2$, $\alpha_2\delta 1$, and $\beta 2a$ ($Ca_v1.2$) in *Xenopus* oocytes induced well characterized inward Ca^{2+}- or Ba^{2+}-$Ca_v1.2$ currents (11, 31, 33, 38). The kinetic properties of $Ca_v1.2$ were recorded in oocytes expressing the three channel subunits along with Sx1A or Sx1A mutant in which both TMD vicinal Cys residues were mutated to Val; C271V/C272V (Sx(CC/VV)) (Fig. 1). Inward currents were evoked from a holding potential of −80 mV in response to a 160-ms voltage step to +20 mV. Current amplitude was significantly inhibited by

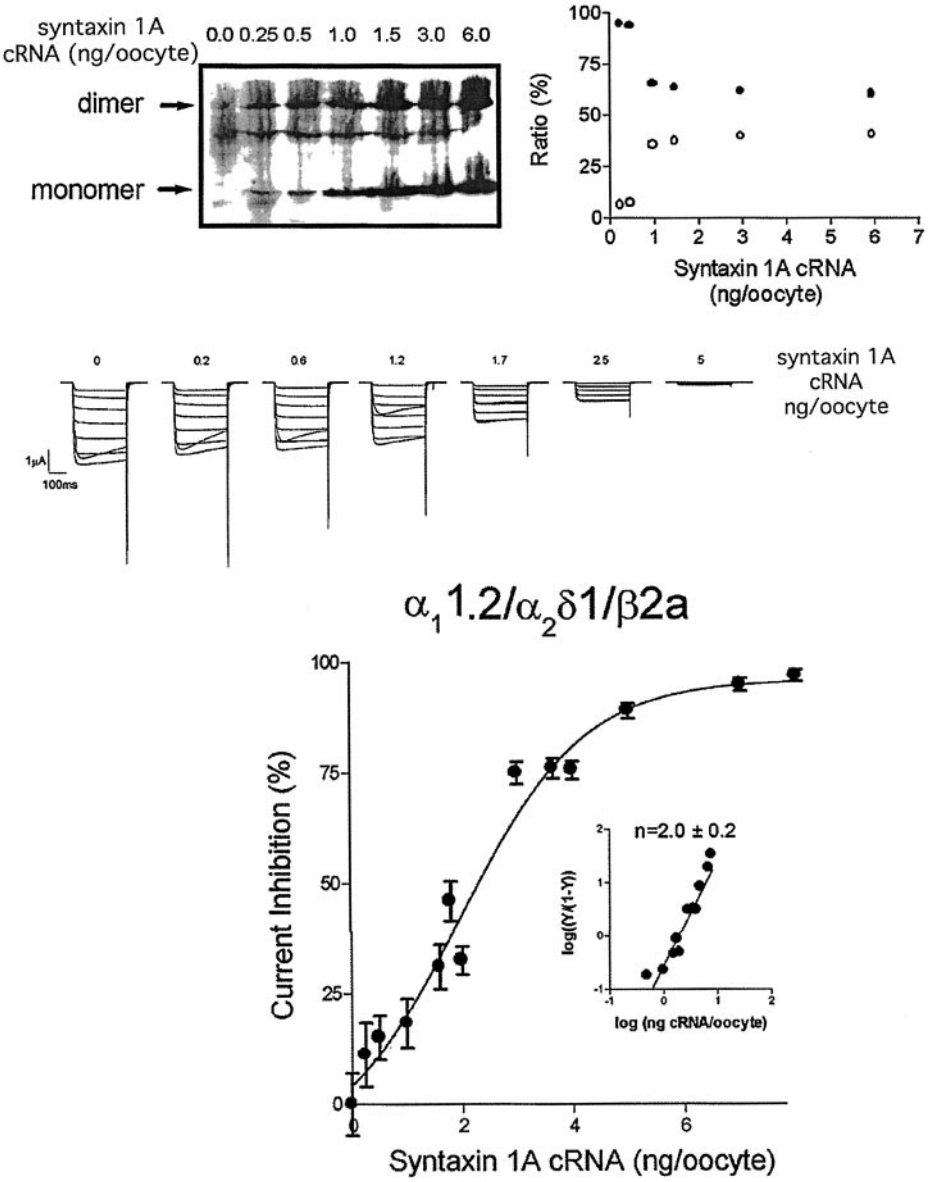

FIG. 4. **Interaction of Sx1A with Lc-type Ca^{2+} channel induces a cooperative current inhibition.** *Xenopus* oocytes were injected with cRNA of channel subunits $\alpha_1$1.2 (2 ng/oocyte), $\alpha_2\delta$1 (1.5 ng/oocyte), and β2a (5 ng/oocyte). Twenty-four hours later, Sx1A cRNA was injected to groups of oocytes (n = 30 in each group) at increasing amounts, as indicated. At day 6, out of each group of 10 oocytes were homogenized, lysed, and separated on 8% SDS-PAGE (see Fig. 2) (*upper panel, left*). The ratio of homodimer and monomer out of the total at each concentration was calculated (*upper panel, right*). Inward currents were recorded from each group of oocytes. Superposition of representative macroscopic Ba^{2+} currents is shown for each Sx1A cRNA concentration in response to a 300-ms test pulse from a holding potential of −80 mV to various potentials (*middle panel*). Normalized peak values of currents were plotted against increasing Sx1A cRNA concentrations (*lower panel*). Each *dot* corresponds to a group of 10–20 oocytes and for most cases S.E. was less than 10% of the averaged values before normalization. *Inset*, Hill plot, calculated from current inhibition. n_H, Hill coefficient was determined from linear regression of the Hill plot.

Sx1A but was not affected by the Sx(CC/VV) mutant (Fig. 1*B*). In contrast, the rate of activation was accelerated to a similar extent by Sx1A and Sx(CC/VV), shown by a decrease in the time constant of activation (τ_{act}) (Fig. 1*C*). Moreover, the mutation in the vicinal cysteines did not interfere with the ability of Sx1A to increase the rate of inactivation as demonstrated in the range of −15 to −5 mV (Fig. 1*D*).

The lack of activity of the Sx1A double mutant pertaining to current amplitude led us to explore the putative role of the vicinal cysteines in Sx1A and homodimer formation.

Transmembranal Cys-271 and Cys-272 of Sx1A Participate in the Homodimerization of Sx1A—Because loss of Sx1A activity was correlated with mutating the two TMD Cys residues, we pursued a biochemical investigation of the potential disulfide bond formation of Sx1A TM domain. For that purpose we have expressed Sx1A and Sx(CC/VV) in *Xenopus* oocytes and tested the appearance of syntaxin homodimers. *Xenopus* oocytes were lysed and suspended in native loading buffer without SDS and DTT, or in a standard buffer containing both. Lysate proteins were then separated on SDS-PAGE and identified by monoclonal anti-Sx1A antibody using a Western blot analysis (Fig. 2*A*). In the absence of DTT, Sx1A appeared both as a monomer and as a homodimer, whereas in the presence of DTT it appeared only as monomer. No homodimers were observed in oocytes expressing Sx(CC/VV) under the same experimental conditions regardless of the presence or absence of DTT in the sample buffer (Fig. 2*A*). An Sx1A mutant Sx(C271V), in which only Cys-271 was mutated to Val, migrated as a homodimer on the gel under native conditions (Fig. 2*C*). Hence, Sx1A homodimer is formed also when a single Cys residue is present at the TM domain. Previously, we showed that this mutant is as active as intact Sx1A (12). These results show a correlation between homodimer formation and Sx1A activity. Furthermore, to the best of our knowledge this represents the first reported native case of formation of disulfide bonds within TM helices.

To test whether the presence of the channel subunits could alter Sx1A dimerization, we examined oocytes injected with $\alpha_1$1.2, $\alpha_2\delta$1, β2a, and Sx1A or Sx(CC/VV). As shown in Fig. 2*B*, Sx1A ran both as a homodimer and a monomer in a gel under native conditions, whereas Sx(CC/VV) was a monomer only. Hence the presence of the channel subunits did not influence Sx1A homodimerization.

Theoretical Model Examining a Disulfide Bond Formation in Sx1A Tail-anchored Helix—Because the formation of membrane-embedded disulfide bonds has not been reported previ-

ously, we have looked at the sequence propensity of the syntaxin TM domains for forming such bonds. As an upper limit for disulfide bond formation, we have set the distance between the respective Cys Sγ (sulfur atom at position γ) to 3.9 Å, noting that in disulfide bonds the distance is 2.1 Å.

A global molecular dynamics search aimed at identifying possible dimeric structures (37) was performed for the TM domains of Sx1A wild type (wt) and each of its mutants, Sx(C271V), Sx(C272V), Sx(C271V, C272V) and in addition syntaxin 2 wt and its mutant Sx2(V272C, V273C) (12). For Sx1A, several possible clusters were found in which the distance between some pairs of cysteines (one on each helix) was 3.54 Å. Specifically, for Sx1A wt, Sγ of Cys-271 on the first helix was away 3.5 Å from Sγ of Cys-272 on the opposing helix.

In addition, clusters with a single possible disulfide bond, either 271/271 or 272/272, were obtained; however, the distance between the respective Sγs was ~3.75 Å. With different combinations of the various mutants, Sγs were found at a distance that varied between 3.54 and 3.89Å (Fig. 3, *a–c*). However, in Sx1A mutants that contained a single Cys residue, the clusters were arranged slightly differently. The clusters maintained their cysteines at a similar distances, such that Sx(C271V) had structures with Sγ distances of 3.35–3.45 Å between their Cys-272 on the two helices. Sx(C272V) had only one structure, in which the distance between the Sγ of the cysteine at position 271 was 3.86 Å.

For syntaxin 2, comparison of average structures resulted in two clusters as follows: one from syntaxin 2 wt, and the other from Sx2(VV/CC) (Fig. 3, *d* and *e*), with an r.m.s.d. <0.3 Å (Fig. 3, *d* and *e*). The resulting structure from Sx2(VV/CC) had a distance of 3.41 Å between Cys Sγ at position 273 from both helices. Its corresponding structure from the wild type sequence had a distance of 3.7 Å between the Cγ of both Val residues. These observations suggest that a disulfide bond can theoretically be generated between two syntaxin TM domains.

Functional Assay Shows a Cooperative Pattern in the Channel Inhibition by Sx1A—The effect of Sx1A concentrations on homodimer formation was studied by injection of increasing concentrations of Sx1A cRNA into oocytes pre-injected 24 h earlier with the three Ca^{2+} channel subunits $\alpha_1$1.2/β2a/α_2δ1. Five to 7 days after cRNA injection, Sx1A protein levels were tested under non-reducing conditions. Densitometry of Sx1A bands showed no saturation of either the monomeric and dimeric forms (data not sown). Because the results of the Western blot and ECL detection analyses are not linear due to the non-linearity of the developing film, we could not determine Sx1A protein concentration by comparing the density of the protein bands (Fig. 4, *upper left panel*). We have therefore limited our analysis to resolving the ratio between Sx1A homodimer and monomer forms, within each lane at each Sx1A concentration (Fig. 4, *upper left panel*). At low levels of Sx1A, abundance of the dimeric form was observed to moderately increase at higher Sx1A concentrations. In contrast, the level of the monomer form was very low at lower Sx1A concentrations (Fig. 4, *upper left panel*). A sharp leap in monomer appearance was noted at cRNA levels of 0.5–1.0 ng/oocyte (Fig. 4, *upper panel*). The ratio obtained showed a constant ratio of 95 to 5% dimer to monomer at low Sx1A levels, and a drastic decrease to 70/30% dimer to monomer, at higher Sx1A cRNA concentration (Fig. 4, *upper right panel*).

This biochemical approach shows Sx1A homodimer as a preferred syntaxin species at low concentration. These results are consistent with the theoretical analysis that demonstrated Sx1A homodimer formation. The appearance of monomers only at higher Sx1A concentrations may exhibit saturation of certain domains permissible for dimer formation, probably due to overexpression. Moreover, homodimerization may increase the hydrophobicity of the tail and, in turn, the efficiency of insertion into membranes. This may prevent inappropriate interac-

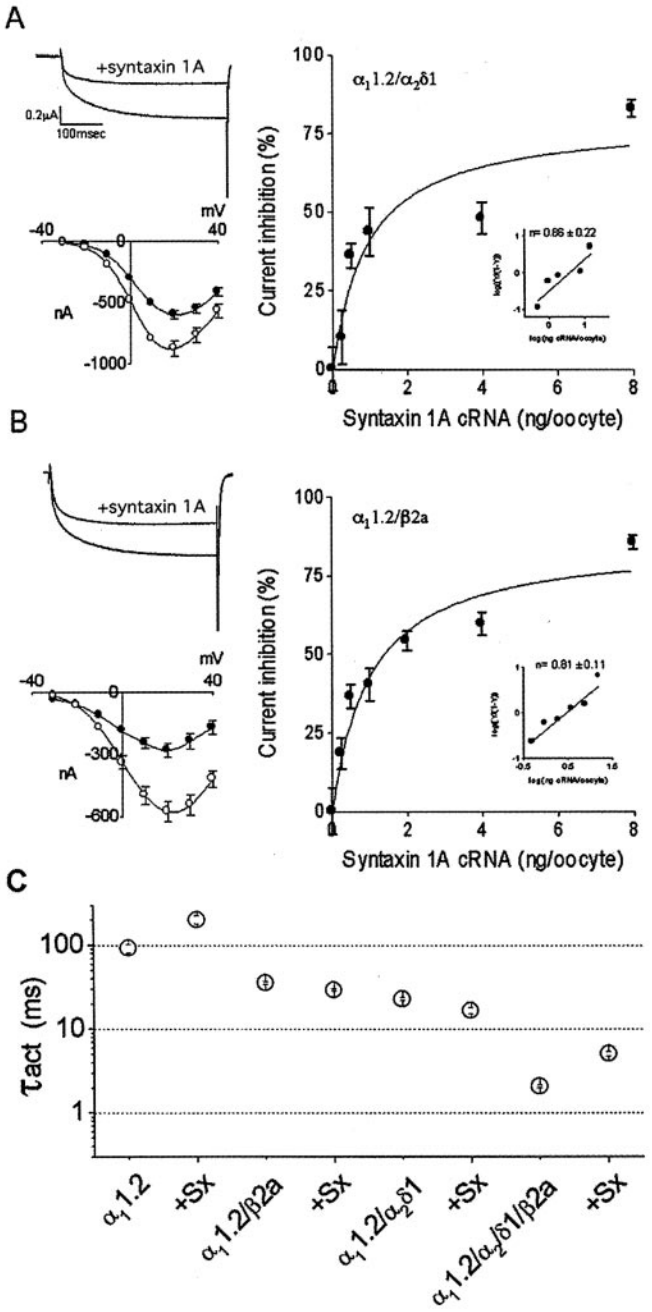

FIG. 5. **Subunit composition of the Ca_v1.2 determines the pattern of current inhibition by Sx1A.** Oocytes were injected with cRNA of channel subunits. *A*, $\alpha_1$1.2/β2a (3 and 5 ng/oocyte, respectively). *B*, $\alpha_1$1.2/$\alpha_2\delta_1$(3 and 2 ng/oocyte, respectively). *A* and *B, right panels,* superposition of representative current traces evoked from a holding potential of −80 mV in response to 400 ms (($\alpha_1$1.2/β2a) or 300 ms ($\alpha_1$1.2/α_2δ1) test pulse to +20 mV of the channel alone and in the presence of Sx1A (2 ng/oocyte). Leak-subtracted peak current-voltage relationship: in the absence (○) or presence of Sx1A (●) (*lower left panels* of *A* and *B*). *A* and *B*, *right panels,* normalized peak Ba^{2+} currents plotted as a function of increasing Sx1A cRNA amounts injected into each group of oocytes (n = 10–20). *Inset,* Hill plots calculated from the results shown on the *left*. Hill coefficients (n_H) were determined from the Hill plots by linear regression. *C*, activation time constants (τ_{act}) derived from single exponential fits of inward currents and plotted against test potential (see "Experimental Procedures" and Table I).

TABLE I

Differential effects of syntaxin 1A on the biophysical properties of $Ca_v1.2$, relative to different subunits composition

Current amplitudes were recorded in 5 mM Ba^{2+} solution (see "Experimental Procedures") in response to depolarizing pulses to: $\alpha_1$1.2 + 30 mV; $\alpha_1$1.2/β2a + 20 mV; $\alpha_1$1.2/$\alpha_2\delta$1 + 20 mV; $\alpha_1$1.2/$\alpha_2\delta$1/β2a + 10 mV. Time constants of activation were analyzed from depolarizing pulses: $\alpha_1$1.2 + 40 mV; $\alpha_1$1.2/β2a + 20 mV; $\alpha_1$1.2/$\alpha_2\delta$1 + 20 mV; $\alpha_1$1.2/$\alpha_2\delta$1/β2a + 10 mV. Syntaxin 1A cRNA injected was 8 ng/oocyte. Hill coefficient is the slope ± S.E. determined by linear regression of the Hill plots.

	Subunit composition							
syntaxin 1A	α_1 1.2		$\alpha_1$1.2/β2a		$\alpha_1$1.2/$\alpha_2\delta$1		$\alpha_1$1.2/$\alpha_2\delta$1/β2a	
	−[a]	+	−	+	−	+	−	+
Peak current amplitude (nA)	−565 ± 51	−41 ± 16	−627 ± 40	−90 ± 12	−937 ± 50	−157 ± 24	−3912 ± 216	−116 ± 24
Hill coefficient n_H		0.87 ± 0.41		0.81 ± 11		0.86 ± 0.22		2.0 ± 0.2
Time constant of activation (ms)	93 ± 10	204 ± 24	35.9 ± 1.4	29.5 ± 0.9	23.0 ± 1.0	16.8 ± 1.4	2.10 ± 0.07	5.15 ± 0.31

[a] − and + refer to syntaxin 1A.

tions of Sx1A with various exocytotic partners until the correct location or condition is achieved.

To test whether the cellular domain permissible for dimer formation interacts with the calcium channels, we have used a functional assay of reconstitution of both proteins (calcium channel and Sx1A) in *Xenopus* oocytes.

Next, we examined which of the syntaxin forms modifies the channel activity. $Ca_v1.2$ currents were recorded in oocytes co-expressing the three subunits $\alpha_1$1.2/β2a/$\alpha_2\delta$1 and Sx1A injected with increasing cRNA concentrations as shown by current traces (Fig. 4, *middle panel*). The peak current amplitude taken from current-voltage relationship of each group of oocytes (n = 10–25) was averaged (S.E. <10%). Current amplitude values were normalized to the control group (with no Sx1A) and plotted against Sx1A cRNA concentration (Fig. 4, *lower panel*). The plot was fitted by a non-Michaelian curve, and analysis of the Hill coefficient (n_H) resulted in n_H = 2.0 ± 0.2 for $Ca_v1.2$ (Fig. 4, *lower panel, inset*) and 1.97 ± 0.12 for the N-type Ca^{2+} channel ($Ca_v2.2$ subunits $\alpha_1$2.2/β2a/$\alpha_2\delta$1; data not shown). The calculated Hill coefficient indicates a cooperative Sx1A effect on $Ca_v1.2$ (Table I) as well as on $Ca_v2.2$. It can be hypothesized that the negligible degree of channel inhibition at low Sx1A concentration indicates that the dimeric form of syntaxin, which is abundant at these low levels, may not be functional species.

Channel Composition Affects Interaction with Sx1A—We have shown previously (11) that Sx1A reduced Ba^{2+} influx through channels composed either of $\alpha_1$1.2, $\alpha_1$1.2/$\alpha_2\delta$1, $\alpha_1$1.2/β2a or $\alpha_1$1.2/β2a/$\alpha_2\delta$1. These results established Sx1A site of action directly at the $\alpha_1$1.2 subunit. Although modification of $\alpha_1$1.2 kinetics indicates a direct interaction with the pore-forming subunit, by incorporating the auxiliary subunits Sx1A interaction is predicted to modify even further, because they change the configuration of $\alpha_1$1.2 and its density at the plasma membranes. Current inhibition by Sx1A was tested with different subunit compositions to explore a requirement of specific channel configuration (Fig. 5, *A–C*). The cRNA encoding $\alpha_1$1.2 subunit was injected by itself or together with either $\alpha_2\delta$1 or β2a cRNAs along with increasing concentrations of Sx1A cRNA using the same cRNA preparation applied in the experiment above (see Fig. 4). Sx1A inhibition was apparent in all subunit combinations as shown by superposition of macroscopic currents, evoked from a holding potential of −80 to +10 mV (Fig. 5, *A* and *B*, *left panel*). Current inhibition by Sx1A was not cooperative in each one of the subunit combinations as illustrated (Fig. 5A, *right panel*; Table I). The degree of inhibition was fitted to a Michaelis-Menten curve with a Hill coefficient of n_H = 0.87 ± 0.41, 0.81 ± 0.11 and 0.86 ± 0.22 for $\alpha_1$1.2 alone or $\alpha_1$1.2/β2a or $\alpha_1$1.2/$\alpha_2\delta$1, respectively. The results indicate that $\alpha_1$1.2 by itself or in conjunction with either of the auxiliary subunits interact with Sx1A in a saturable Michaelis-Menten manner (Fig. 5, *A* and *B*) as opposed to the non-linear curve obtained when all three subunits were present (Fig. 4). We also analyzed the effect of subunit composition on the activation time constants (τ_{act}) of $\alpha_1$1.2 subunit injected with each one of the subunit combinations (Fig. 5*C* and Table I). Co-expression of the auxiliary subunit β2a or $\alpha_2\delta$1 increased $\alpha_1$1.2, activation by 3- and 4-fold, respectively, consistent with an intrinsic

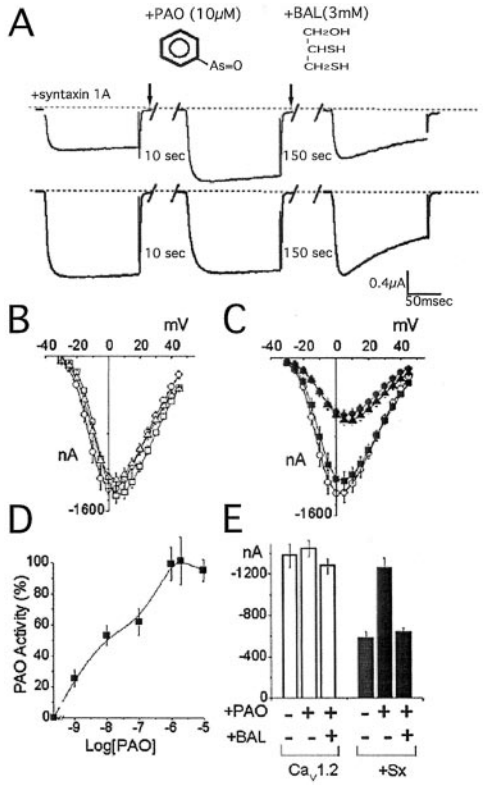

FIG. 6. **PAO abrogates the Sx1A inhibitory effect of $Ca_v1.2$ activity and BAL reverses PAO action.** *A*, *left panel*, Ba^{2+} currents were activated from a holding potential of −80 mV by a single voltage step of 140-ms duration to a step potential of +20 mV in oocytes expressing $\alpha_1$1.2/$\alpha_2\delta$1/β2a subunits with (*upper panel*) or without Sx1A (*lower panel*). Then PAO (10 μM) was applied to the bath and after 10 s currents were recorded (*middle*). Two min later, BAL (0.3 mM) was applied for 2.5 min, and currents were activated as described above (*right*). *B*, leak-subtracted peak current-voltage relationship: collected data from oocytes expressing the three channel subunits (○) incubated for 10 s with 10 μM PAO (□) and then with 0.3 mM BAL ([trio]). *C*, same as *B* in oocytes expressing the three channel subunits along with Sx1A (●), incubated for 10 s with 10 μM PAO (■), and then with 0.3 mM BAL (▲). The data points correspond to the mean ± S.E. of current amplitude (n = 7). *D*, a dose-response curve for reversal of Sx1A effect was determined at PAO range of 1 nM and 0.1 mM. *E*, current amplitudes evoked in oocytes expressing the three channel subunits and oocytes expressing the channel subunits along with Sx1A (data of Fig. 2, *B* and *C*). Currents amplitudes were decreased by Sx1A and reversed by PAO, whereas BAL abolished the PAO effect. Current amplitudes evoked in oocytes expressing only the channel subunits were not affected by either one of the reagents. The data correspond to the mean ± S.E. of current amplitude (n = 8, Table III).

TABLE II
PAO and BAL activity on syntaxin 1A

Peak currents were recorded in response to depolarization steps to +20 mV. $V_{1/2}$ mg (midpoint of activation) and slope were determind from regression analysis of the current-voltage relationship plots. Sx, syntaxin.

	$Ca_v1.2$				+Sx			
	Peak	$V_{1/2}$	Slope	*n*	Peak	$V_{1/2}$	Slope	*n*
	nA	*mV*			*nA*	*mV*		
5 mM Ba^{2+}	−1376 ± 114	−13.0 ± 0.6	−4.4 ± 0.2	12	−583 ± 61[a]	−10.6 ± 0.7[b]	−5.8 ± 0.2[a]	10
+10 μM PAO	−1444 ± 77	−8.8 ± 0.5[a]	−4.7 ± 0.1	8	−1252 ± 96	−11.4 ± 0.7	−4.5 ± 0.2	15
+10 μM PAO 3 mM BAL	−1278 ± 72	−11.2 ± 1.0	−4.4 ± 0.2	6	−645 ± 50[a]	−9.7 ± 1.0[b]	−6.2 ± 0.2[a]	7
5 mM Ca^{2+}	−781 ± 76	−6.6 ± 1.3	−7.0 ± 0.4	8	−497 ± 55[b]	−0.2 ± 0.7[b]	−7.8 ± 0.1	11
+1 μM PAO	−739 ± 68	1.4 ± 0.6[a]	−8.0 ± 0.3	3	−856 ± 93	−0.5 ± 0.6[b]	−7.8 ± 0.2	5
+1 μM PAO 0.1 mM BAL	−1081 ± 127	2.9 ± 0.8[a]	−7.0 ± 0.5	3	−462 ± 62[b]	3.5 ± 0.7[a]	−8.6 ± 0.5	8

[a] $p < 0.001$.
[b] $p < 0.02$.

change in channel gating that accompanies the apparent increase in current density. The indicated difference in channel conformation induced by the assembly of channel subunits was also apparent by a modified effect of Sx1A on the activation rate. Whereas Sx1A reduced the activation of $\alpha_1$1.2 expressed alone or together with both auxiliary subunits (31, 33), a small but significant increase in the activation was observed in $\alpha_1$1.2 co-expressed with only one of the auxiliary subunits (Fig. 5*C* and Table I).

Selective and Reversible Inactivation of Thiol Group Reactivity of Sx1A—To verify that Sx1A monomer is the functional form, we have set up a functional assay to differentiate dimers from monomers by selectively modifying the Sx1A monomers.

PAO is a thiol reagent that selectively reacts with vicinal Cys residues (39). It forms a stable complex with vicinal thiol groups, compared with adducts formed with a single cysteine. PAO was applied directly into the recording bath of oocytes co-expressing either the channel alone or along with Sx1A. At first, inhibition of current amplitude was monitored in an oocyte prior to addition of PAO (Fig. 6*A*, *upper left panel*). The oocyte was then exposed to 10 μM PAO for 10 s, and currents were recorded. Inhibition was abolished, as amplitude in the presence of PAO was back to control amplitude in oocytes without Sx1A (Fig. 6*A*, *middle upper*). PAO had no effect on current amplitude in oocytes expressing the three channel subunits (Fig. 6*A*, *middle lower*). Then the same oocyte was exposed to 3 mM 2,3-dimercaptopropanol (British anti-Lewisite (BAL), a PAO antidote, for 2.5 min. As shown in Fig. 6*A*, *right upper*, BAL reversed the PAO effect, and the inhibition of current amplitude was re-established, to the same extent as that obtained prior to PAO application (Table II). It should be noted that BAL, independent of its effect on reversing the PAO effect, accelerated the inactivation of the channel (Fig. 6*A*, *right*).

As a thiol reagent, reversal of Sx1A inhibition of current amplitude could be due to chemical PAO modification of vicinal thiol groups at the Sx1A TM domain. Collected data from oocytes expressing the three channel subunits and Sx1A that were exposed for 10 s to PAO and 2.5 min to BAL according to the protocol described for a single oocyte (above) is shown as leak-subtracted peak current-voltage relationship (Fig. 6*C*; Table II). To ascertain that PAO addition followed by BAL had no effect on the channel properties, 10 μM PAO and 10 μM PAO combined with 0.3 mM BAL were added to oocytes injected only with the three channel subunits. As shown in Fig. 6*B,* the current-voltage relationships of the channel were affected neither by PAO nor PAO combined with BAL. Reversal of Sx1A inhibition in a dose-dependent manner was established in a PAO range of 1 nM to 0.1 mM as indicated (Fig. 6*D*).

The results of four experiments demonstrating Sx1A inhibition of current amplitude, PAO reversal of Sx1A effect, and the return of the effect by BAL are summarized in Fig. 6*E*. Similar results were obtained when Ba^{2+} was switched to Ca^{2+} (Table II). PAO was less effective at reversing current inhibition induced by the Sx1A mutant Sx(C271V) (Table III). These results are consistent with a more labile bond formed between PAO and single thiol group.

DISCUSSION

In this study we have investigated several aspects of Sx1A regulation of Ca^{2+} channel activity reconstituted in *Xenopus* oocytes. We showed that Sx1A inhibition of $Ca_v1.2$ (Lc-type channel) currents is dependent on cysteine residues Cys-271 and Cys-272 located at the Sx1A TMD. Mutation of the two Cys residues to Val in the Sx1A double mutant ((Sx(CC/VV)) abolished the modulation of Ca^{2+} current amplitude. In contrast, Sx(CC/VV) similar to Sx1A wt, accelerated $Ca_v1.2$ kinetics, and to a certain extent channel inactivation. Consistent with our previous studies, when Ca^{2+} is the charge carrier, Sx1A accelerates the activation, as opposed to Ba^{2+} activation that is slowed down (33). Although essential, the Cys residues are not sufficient for conferring inhibition of current amplitude because a chimeric syntaxin 2 containing Sx1A TMD does not inhibit ion currents (12). Moreover, cleavage of Sx1A by botulinum toxin C1 close to the TMD at amino acid 253/254 (40) partially uncouples the syntaxin-channel interface, in turn abolishing inhibition of current amplitude (12). In contrast, in both experiments the Sx1A effect on channel activation was apparent, indicating that the cytosolic region of Sx1A contains channel interacting domains that contribute both to kinetic modulation and channel inhibition. The sequence specificity of the TMD is critical and greatly influences current amplitude. In contrast, TMD sequence alterations can be tolerated without alteration of $Ca_v1.2$ activation and inactivation, consistent with C-terminal mutations that do not alter the Sx1A effect on N-type channel inactivation (41).

In view of the essential role played by TMD Cys-271 and Cys-272 of Sx1A, we explored disulfide bond formation, although sulfhydryl groups within transmembrane helices of membranous proteins, to the best of our knowledge, have not been observed. Sx1A homodimers were apparent by gel electrophoresis with no SDS in the homogenization buffer and under non-reducing conditions. In contrast, the double mutant, Sx(CC/VV) in which the two Cys residues were mutated appeared only as a monomer. Interestingly, homodimer were generated by Sx1A mutant Sx(C271V) in which only one Cys was present.

Because the TMD Cys residues are essential for dimer formation as well as Sx1A activity, we tested the theoretical likelihood of disulfide bonds within Cys residues at the tail-anchored helices of two adjacent Sx1A molecules.

A global molecular dynamic search (37) has been performed

TABLE III
PAO and BAL actvity on Sx(C271V)

Peak currents were recorded in solution containing 5 mM Ba^{2+} in response to depolarization steps to +20 mV. $V_{1/2}$ mg (midpoint of activation) and slope were determind from regression analysis of the current-voltage relationship plots. PAO and BAL concentrations were 1 μM and 0.1 mM respectively.

	Peak	$V_{1/2}$ mg	Slope	*n*
	nA	*mV*		
$Ca_v1.2$	−1186 ± 184	−8.7 ± 1.0	−4.8 ± 0.4	4
+Sx(C271V)	−690 ± 101[a]	0.8 ± 0.9[b]	−5.9 ± 0.3[a]	4
+Sx(C271V) + PAO	−841 ± 84	−0.9 ± 0.2[b]	−6.2 ± 2.7	4
+Sx(C271V) + PAO + BAL	−492 ± 67[a]	−3.2 ± 1.8[a]	−8.3 ± 0.7[a]	5

[a] $p < 0.05$.
[b] $p < 0.005$.

for Sx1A wt and each of its mutants: Sx(C271V), Sx(C272V), and Sx(CC/VV) and, in addition, the TM domain of syntaxin 2 wt and its mutant Sx2(VV/CC) in which Val-272 and Val-273 were mutated to Cys residues (12). These theoretical calculations examined the distances between the Cys Sγ, whereby constraints for such a bond involves proximity of 3.4 and 3.9 Å. The two vicinal cysteines of Sx1A could form two disulfide bonds with distances of 3.58 and 3.54 Å for their Sγs or a single disulfide bond of 3.75 Å. The single Cys mutants and syntaxin 2 mutants Sx2(V272C and V273C) could also form homodimers. Thus, the global molecular dynamic calculations established the feasibility of disulfide bond formation between Cys residues of syntaxin TMD helices, consistent with homodimers of Sx1A that were obtained biochemically.

Next we examined whether syntaxin homodimers are the active species acting to modify the channel by monitoring the ratio of dimer to monomer. The density ratio of dimers *versus* monomers at increasing Sx1A concentrations was highest at low Sx1A concentration, whereas Sx1A activity at low Sx1A concentration was minimal. Sx1A action on current amplitude soared sharply in a non-linear fashion in correlation with the sharper increase in monomer/dimer ratio. This pattern strongly suggests that the monomer and not the homodimer is the active species.

To substantiate Sx1A monomer as the active interacting moiety, we used a thiol-reactive agent. PAO is a selective trivalent arsenical reagent that forms stable ring complexes with vicinal dithiols (39). An immediate relief of the Sx1A inhibition after PAO application to oocytes expressing Sx1A indicates blocking of the Sx1A vicinal Cys residues. The immediate reversal of Sx1A inhibition and the restoration of its effect by BAL strongly suggests that TMD thiol group is the interacting species and that TMD Cys residues play a crucial role in the cross-talk with the voltage-gated calcium channel. It is also consistent with Sx1A direct interaction with the channel, rather than an indirect effect on channel trafficking to the cell membrane. Thus, the PAO experiment further supports the Sx1A monomer as the active species because a cysteine-bridged dimer has at best only one accessible thiol group. We can speculate from the PAO preference to vicinal Cys that the orientation of Sx1A TMD toward a yet unknown interacting domain at the Ca^{2+} channel may leave the two cysteines accessible for reacting with PAO.

The fact that Sx1A is found as a non-functional oligomer in the membrane is not without precedence. As an example, phospholamban, a small bitopic membrane-protein from cardiac sarcoplasmic reticulum, is a known inhibitor of the resident Ca^{2+}-ATPase (42). Despite the fact that phospholamban forms homo-pentamers due to its transmembrane domain, the monomer is thought to be the active species. Thus, the pentamer serves as an inactive reservoir of inhibitory molecules that dissociate to active monomers. Interestingly, phospholamban also contains several cysteine residues in its transmembrane

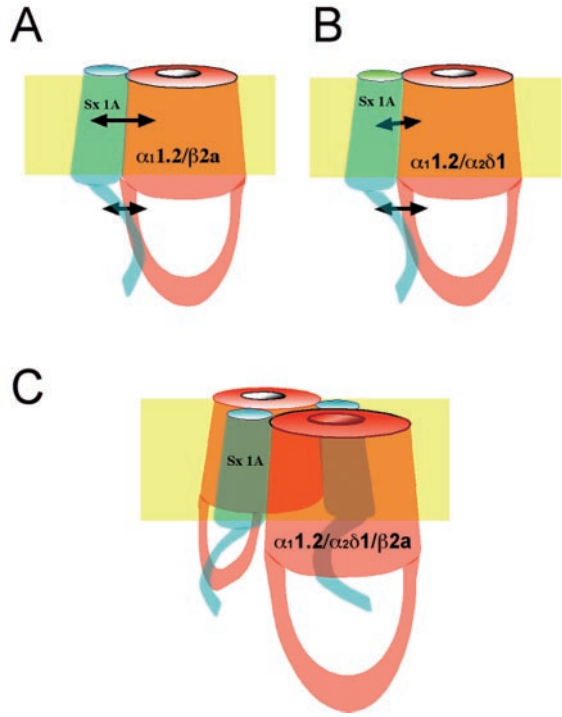

FIG. 7. **Schematic models illustrating possible non-linear mechanisms for Sx1A action on Ca^{2+} channels.** *A*, a conducting channel composed of $\alpha_1 1.2/\beta 2a$ subunits interacts with Sx1A at two putative sites and displays non-cooperative current inhibition. *B*, a conducting channel composed of $\alpha_1 1.2/\alpha_2\delta 1$ subunits interacts with Sx1A at two putative sites and displays non-cooperative current inhibition. *C*, a conducting channel composed of the three channel subunits $\alpha_1 1.2/\alpha_2\delta 1/\beta 2a$ interacts with Sx1A in a non-linear way, which could fit an interaction of Sx1A with a dimer of a three-subunit channel. At lower concentrations, Sx1A binds at two independent sites with relatively low affinity and mildly reducing channel activity. At higher concentrations, a second molecule would interact with higher affinity, causing a large reduction of inward currents. From the Hill coefficients, at least two channels could be associated to form a cluster, each one can bind a single Sx1A, and binding of the first Sx1A molecule would affect the affinity of additional Sx1A molecules to the complex.

domain, albeit non-vicinal, but none have been implicated in forming a disulfide bond in the process of pentamerization. Also, the homodimer of synaptobrevin presumably has no functional role *in vivo* (43).

Inhibition of inward currents through voltage-gated Ca^{2+} channels was observed to be non-linear with increasing Sx1A concentrations for both $Ca_v1.2$ (using del1733Lc) and $Ca_v2.2$. The supralinearity, based on a dose-dependent inhibition, was estimated using the Hill equation to be close to 2 for both channel types. This non-linear relationship indicates either a single channel interaction with more than two Sx1A molecules or a cluster of more than two channels, each one interacting with a single syntaxin molecule. These two possibilities are

schematically illustrated in Fig. 7. According to the model, while a two-subunit channel exhibits a saturable interaction with Sx1A (Fig. 7, *A* and *B*), three subunits would form a cluster of channels (Fig. 7*C*), demonstrating a steep, non-linear relationship with Sx1A.

Various studies of calcium channels have shown the importance of channel auxiliary subunits for correct targeting to the plasma membrane in addition to modulation of channel kinetics (19, 20, 44–47). It was also suggested that the signal necessary for correct plasma membrane targeting of Lc-type calcium channel complexes is generated as a result of a functional interaction between the α_1 and β subunits (21, 48). Here we showed that Sx1A inhibition is strongly affected by the channel subunit composition. Modulation of current amplitude appeared non-cooperative in the absence of $\alpha_2\delta1$ or $\beta2a$ and showed significantly slower activation. In contrast, the heterotrimeric channel was effectively inhibited by Sx1A in a cooperative manner and displayed the fastest rate of activation (Table I). Moreover, Sx1A increased the activation of a two-subunit channel rather than a decrease observed in a three-subunit channel. Such modification by Sx1A on activation rate is consistent with changes in channel conformation during subunit assembly.

Furthermore, because the PAO studies suggest that the monomer is most likely the reactive species, a cooperative change in the inhibition by Sx1A could be the result of at least two channel heterotrimers ($\alpha_1$1.2/α 2δ1/β2a) that interact with Sx1A. It is well established that a functional channel will be targeted to the membrane when assembled with all the channel subunits. A higher density of channels increases the probability of Sx1A encountering a dimer of a channel. Furthermore, a structure of skeletal L-type calcium channel consisting of the three channel subunits in a 25-Å resolution showed a dimeric organization of the channel (49). Such an association, if applicable to the cardiac channel, could explain an allosteric modulation of the channel by Sx1A. The first Sx1A molecule binds to a channel dimer (a dimer of a heterotrimer) affecting the binding of a second Sx1A molecule. An allosteric regulation was established previously for a dimer of aspartate *trans*-carbamoylase trimer, where the binding of a second molecule of aspartate is stronger (50). An alternative difference in the channel interaction with two Sx1A molecules could be due to interaction of TMD and cytosolic domains of syntaxin. When one of the channel auxiliary subunits is missing, one of the interaction interface sites might be less accessible, and therefore Sx1A inhibition becomes non-cooperative.

In summary, Sx1A modifies Ca^{2+} channel kinetics through the cytosolic domain and two cysteines located at the TMD. Although theoretically a disulfide bond can be generated between two TMD helices of Sx1A, and biochemically Sx1A does form homodimers, modulation of the current amplitude of the voltage-gated calcium channels is mediated by Sx1A monomer. The possibility that Ca^{2+} channels exist as dimers of trimers (or tetramers) at the cell membrane (49) could explain a cooperative inhibition by Sx1A monomer. Neurotransmitter release is well established as a cooperative process that depends on Ca^{2+} entry through voltage-gated calcium channels (51). It was also shown that SNARE proteins are important for determining the cooperative relationship between Ca^{2+} and synaptic transmission (52). In addition, conformational changes at the Ca^{2+} channel that occur during membrane depolarization and transduced to Sx1A were suggested to initiate the release process (13, 33, 34, 53). Therefore, the cooperativity in channel/Sx1A interaction shown in the present study may well contribute to the non-linearity of the release process.

REFERENCES

1. Sollner, T., Bennett, M. K., Whiteheart, S. W., Scheller, R. H., and Rothman, J. E. (1993) *Cell* **7,** 5409–5418
2. Rothman, J. E. (1994) *Nature* **372,** 55–63
3. Sutton, R. B., Fasshauer, D., Jahn, R., and Brunger, A. T. (1998) *Nature* **395,** 347–353
4. Poirier, M. A., Hao, J. C., Malkus, P. N., Chan, C., Moore, M. F., King, D. S., and Bennett, M. K. (1998) *J. Biol. Chem.* **273,** 11370–11377
5. Lewis, J. L., Dong, M., Earles, C. A., and Chapman, E. R. (2001) *J. Biol. Chem.* **276,** 15458–15465
6. Margittai, M., Otto, H., and Jahn, R. (1999) *FEBS Lett.* **446,** 40–44
7. Kutay, U., Ahnert-Hilger, G., Hartmann, E., Wiedenmann, B., and Rapoport, T. A. (1995) *EMBO J.* **14,** 217–223
8. Bulbarelli, A., Sprocati, T., Barberi, M., Pedrazzini, E., and Borgese, N. (2002) *J. Cell Sci.* **115,** 1689–1702
9. Laage, R., and Langosch, D. (1997) *Eur. J. Biochem.* **249,** 540–546
10. Laage, R., Rohde, J., Brosig, B., and Langosch, D. (2000) *J. Biol. Chem.* **275,** 17481–17487
11. Wiser, O., Bennett, M. K., and Atlas, D. (1996) *EMBO J.* **15,** 4100–4110
12. Trus, M., Wiser, O., Goodnough, M. C., and Atlas, D. (2001) *Neuroscience* **104,** 599–607
13. Atlas, D., Wiser, O., and Trus, M. (2001) *Cell. Mol. Neurobiol.* **21,** 717–731
14. Shistik, E., Ivanina, T., Puri, T., Hosey, M., and Dascal, N. (1995) *J. Physiol.* (*Lond.*) **489,** 55–62
15. Mitterdorfer, J., Froschmayr, M., Grabner, M., Striessnig, J., and Glossmann, H. (1994) *FEBS Lett.* **352,** 141–145
16. Mastrogiacomo, A., Parsons, S. M., Zampighi, G. A., Jenden, D. J., Umbach, J. A., and Gundersen, C. B. (1994) *Science* **263,** 981–982
17. Kamp, T. J., Perez-Garcia, M. T., and Marban, E. (1996) *J. Physiol.* (*Lond.*) **492,** 89–96
18. Gurnett, C. A., and Campbell, K. P. (1996) *J. Biol. Chem.* **271,** 27975–27978
19. Walker, D., and De Waard, M. (1998) *Trends Neurosci.* **21,** 148–154
20. Brice, N. L., and Dolphin, A. C. (1999) *J. Physiol.* (*Lond.*) **515,** 685–694
21. Leveque, C., Pupier, S., Marqueze, B., Geslin, L., Kataoka, M., Takahashi, M., DeWaard, M., and Seagar, M. (1998) *J. Biol. Chem.* **273,** 13488–13492
22. Gao, T., Chien, A. J., and Hosey, M. M. (1999) *J. Biol. Chem.* **274,** 2137–2144
23. Mirotznik, R. R., Zheng, X., and Stanley, E. F. (2000) *J. Neurosci.* **20,** 7614–7621
24. Jarvis, S. E., and Zamponi, G. W. (2001) *J. Neurosci.* **21,** 2939–2948
25. Hibino, H., Pironkova, R., Onwumere, O., Vologodskaia, M., Hudspeth, A. J., and Lesage, F. (2002) *Neuron* **34,** 411–423
26. Sheng, Z. H., Rettig, J., Takahashi, M., and Catterall, W. A. (1994) *Neuron* **13,** 1303–1313
27. Rettig, J., Sheng, Z. H., Kim, D. K., Hodson, C. D., Snutch, T. P., and Catterall, W. A. (1996) *Proc. Natl. Acad. Sci. U. S. A.* **93,** 7363–7368
28. Bezprozvanny, I., Scheller, R. H., and Tsien, R. W. (1995) *Nature* **378,** 623–626
29. Wiser, O., Tobi, D., Trus, M., and Atlas, D. (1997) *FEBS Lett.* **404,** 203–207
30. Tobi, D., Wiser, O., Trus, M., and Atlas, D. (1998) *Receptors Channels* **6,** 89–98
31. Wiser, O., Trus, M. A., Hernandez, A., Renstrom, E., Barg, S., Rorsman, P., and Atlas, D. (1999) *Proc. Natl. Acad. Sci. U. S. A.* **96,** 248–253
32. Catterall, W. A. (1999) *Ann. N. Y. Acad. Sci.* **868,** 144–159
33. Wiser, O., Cohen, R., and Atlas, D. (2002) *Proc. Natl. Acad. Sci. U. S. A.* **99,** 3968–3973
34. Atlas, D. (2001) *J. Neurochem.* **77,** 972–985
35. Brunger, A., Adams, P., Clore, G., Gros, W., Grosse-Kunstleve, R., Jiang, J., Kuszewski, J., Nilges, M., Pannu, N., Read, R., Rice, L., Simonson, T., and Warren, G. (1998) *Acta Crystallogr. Sect. D Biol. Crystallogr.* **5,** 905–921
36. Jorgensen, W., and Tirado-Rives, J. (1998) *J. Am. Chem. Soc.* **110,** 1657–1666
37. Adams, P., Arkin, I., Engelman, D., and Brunger, A. (1995) *Nat. Struct. Biol.* **2,** 154–162
38. Singer, D., Biel, M., Lotan, I., Flockerzi, V., Hofmann, F., and Dascal, N. (1991) *Science* **253,** 1553–1557
39. Frost, S. C., and Lane, M. D. (1985) *J. Biol. Chem.* **260,** 2646–2652
40. Schiavo, G., Shone, C. C., Bennett, M. K., Scheller, R. H., and Montecucco, C. (1995) *J. Biol. Chem.* **270,** 10566–10570
41. Bezprozvanny, I., Zhong, P., Scheller, R. H., and Tsien, R. W. (2000) *Proc. Natl. Acad. Sci. U. S. A.* **97,** 13943–13948
42. Frank, K., and Kranias, E. G. (2000) *Ann. Med.* **325,** 72–78
43. Bowen, M. E., Engelman, D. M., and Brunger, A. T. (2002) *Biochemistry* **41,** 15861–15866
44. Wyatt, C. N., Page, K. M., Berrow, N. S., Brice, N. L., and Dolphin, A. C. (1998) *J. Physiol.* (*Lond.*) **510,** 347–360
45. Yamaguchi, H., Hara, M., Strobeck, M., Fukasawa, K., Schwartz, A., and Varadi, G. (1998) *J. Biol. Chem.* **273,** 19348–19356
46. Hofmann, F., Lacinova, L., and Klugbauer, N. (1999) *Rev. Physiol. Biochem. Pharmacol.* **139,** 33–87
47. Striessnig, J. (1999) *Cell. Physiol. Biochem.* **9,** 242–269
48. Catterall, W. A. (2000) *Annu. Rev. Cell Dev. Biol.* **16,** 521–555
49. Wang, M., Velarde, G., Ford, R., Berrow, N., Dolphin, A., and Kitmitto, A. (2002) *J. Mol. Biol.* **323,** 85–98
50. Gerhart, J. C., and Schachman, H. K. (1965) *Biochemistry* **4,** 1054–1062
51. Dodge, F. A., Jr., and Rahamimoff, R. (1967) *J. Physiol.* (*Lond.*) **193,** 419–432
52. Stewart, B. A., Mohtashami, M., Trimble, W. S., and Boulianne, G. L. (2000) *Proc. Natl. Acad. Sci. U. S. A.* **97,** 13955–13960
53. Cohen, R., Elferink, L. A., and Atlas, D. (2003) *J. Biol. Chem.* **278,** 9258–9266